Journal of Natural Sciences,
Life and Applied Sciences
Issue (4), Volume 1
December 2017
ISSN: 2518-5780

المجلة العربية للعلوم و نشر الأبحاث
Arab Journal of Sciences & Research Publishing
AJSRP

Solvatochromism Effect Studies on Electronic Absorption Spectral of Some Hydroxy Tolyl Azo Benzaldehyde dyes.

Asma M. Al Jebaly **Sokaina S. Hemdan** **Fatma K. Ali**
Chemistry Department || Factually of Science and Art El Marj || Benghazi University || El Marj || Libya

ABSTRACT: The electronic absorption spectra of some prepared substituted aryl azo compounds were recorded in organic solvents of different polarities. The electronic transitions are assigned. The solvents and substituents effects on the spectral behaviour are studied and interpreted. The solvent induced spectral effects have been analyzed using multiple linear regression technique. The Kamlet-Taft and Catalan's solvent scales were found to be the most suitable for describing the solvatochromic shifts of the absorption spectra. The solute–solvent interactions were determined based on multilinear solvation energy relationships concept. The phenomena of tautomersim were discussed with the possibility of forming intra and intermolecular hydrogen bonds.

KEY WORDS: Azo Dyes, Absorption Spectra, Organic Solvents, Multiple linear regressions.

INTROUDUCTION

Azo group is concerned with a number of important biological reactions (1) such as a protein synthesis inhibition, carcinogenesis, azo reduction monoamines oxides inhibitions, immunochemical affinity labelling and nitrogen fixation and histochemical detection of compounds containing –**SH** group (2). The presence of donor and acceptor substituents in the conjugated systems of the dye can be of interest in the study of solvent and substituent effects on the **UV-Vis** spectroscopic absorption maxima, λ_{max}, of the azobenzene dyes. In addition, the planarity of the azo link contrast with the other part of the system should allow larger π electron transmission and lead to higher optical activity (3). UV-Visible spectrophotometry is the fundamental and most widely spread method for the qualitative and quantitative analysis of organic compounds, whereas spectra fluorometry involves the measurement of emitted light by a molecule following **UV** light excitation. The absorption or emission spectral curves are dependent on the solvent media (4). Application of the techniques of multiple linear regressions has proved to be exotically successful and has greatly improved the understanding of the solvent role (5).

Their **UV–Vis** absorption spectra can be influenced by non-specific interactions such as ion–dipole, dipole–dipole (Keesom interaction), induced dipole–permanent dipole interactions (Debye interaction) or by specific interaction such as hydrogen bonding with solvents. Thus, solvents play an important role in physical and chemical processes and can determine change in the position, intensity, and shape of absorption bands (6). Specific interactions can be present in solutions, the most important ones being hydrogen bonding (7). Their influence on the absorption spectra is very important, depending on whether the solvent molecules can act as donors or acceptors in the formation of hydrogen bonding with the solute molecules. Solvatochromism is a powerful tool technique to investigate the physical–chemical properties of molecules (8).

OBJECTIVE OF THE STUDY

The Aim of this study is to investigate the effect of solvent influence on the **UV–Vis** absorption spectra of some highly colored hydroxy benzaldehyde azo dyes were prepared, **(Scheme I)**, where these compounds absorb due to extensive conjugation of the azo group with the aromatic rings. The spectral characteristics of the studied azo molecules in nine different solvents at room temperature were analyzed in this paper. SPSS **(program of statistical package of social sciences) version 17** has been used to determine coefficients by multiple linear regression technique.

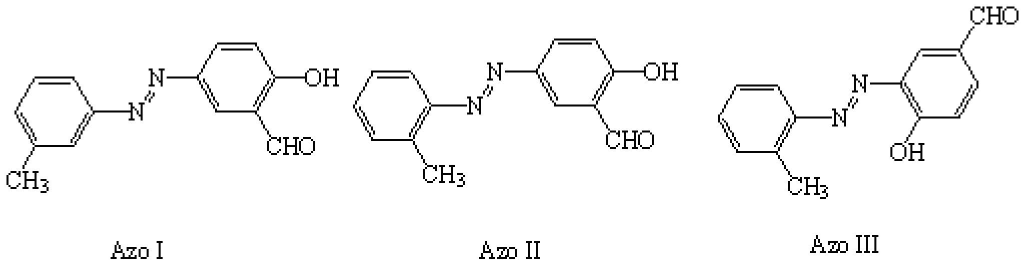
Azo I Azo II Azo III

Scheme (I): Molecular Structure for studied azo dyes (10).

EXPERIMENTAL

In study, **2**-hydroxy-5(E)[(3-methylphenyl) diazneyl]benzaldehyde, **2**-hydroxy-5(E)[2-methyl phenyl) diazenyl] benzaldehyde, and **4**-hydroxy-3-[(E)-(2-methyl phenyl) ,**(Scheme I),** compounds were synthesized as indicated in the literature(9) by Al Jebaly (10).

UV/Vis absorption spectral measurements were recorded for each azo dye in the proper solvent with CECIL – CE 7400(S.n.146368, England) UV-Visible Spectrophotometer covering the wavelength range 250-600 nm with a 1-cm path length quartz cell was used for UV–Vis spectra acquisition at room temperature *(~20 °C).* Nine different solvents namely 1,4-dioxane *(Dix)*, ethanol *(EtOH)*, methanol *(MtOH)*, 1-propanol *(PrOH)*, n-hexane*(HE)*, ethyl acetate *(EtAC)*, deionized water *(*H_2O*)*, Dimethyl sulphoxide *(DMSO)* and Acetone *(AC)* were used without further purification for spectroscopic grade. These solvents have different polarity parameters *(E, K, M, J, H and N)*, mainly related to the refractive index *n* and dielectric constant ε of each solvent (11-14). The solvatochromic parameters (π^*, α and β) were taken from literature (15,6) and Catalân parameters were taken from the literature (16, 17). The physical parameters for the solvents at **~20 °C** are collected in **Table (1)** below, in which the solvents are arranged in the order of increasing polarity.

Table (1): Solvent Parameters used in the Spectral Correlation Equations.

Solvents /Parameter	*HE*	*Dix*	*EtAc*	*MtOH*	*EtOH*	*PrOH*	*AC*	*DMSO*	*H_2O*
n	1.3748	1.422	1.3723	1.3288	1.3611	1.3855	1.3588	1.4787	1.3333
ε	1.890	2.222	6.080	33.10	24.30	20.80	21.10	47.24	78.50
K	0.188	0.223	0.385	0.477	0.470	0.464	0.465	0.485	0.491
M	0.186	0.203	0.185	0.169	0.181	0.190	0.180	0.221	0.171
N	0.0019	0.031	0.398	0.710	0.665	0.630	0.648	0.658	0.757
E	30.90	36.00	38.10	55.50	51.90	50.70	42.20	45.00	63.10
J	0.231	0.286	0.625	0.913	0.886	0.864	0.868	0.941	0.963
H	0.229	0.254	0.228	0.203	0.221	0.235	0.220	0.283	0.206
α	0.000	0.000	0.000	0.930	0.830	0.780	0.080	0.000	1.170
β	0.000	0.370	0.450	0.620	0.770	0.850	0.480	0.760	0.470
$\pi*$	−0.081	0.550	0.540	0.60	0.540	0.520	0.710	1.000	1.090
SA	0.000	0.000	0.000	0.605	0.400	0.367	0.000	0.072	1.062
SB	0.056	0.444	0.542	0.545	0.658	0.782	0.475	0.647	0.025
SdP	0.000	0.312	0.603	0.904	0.783	0.748	0.907	1.000	0.997
SP	0.616	0.737	0.656	0.608	0.633	0.658	0.651	0.830	0.681

RESULTS AND DISCUSSION

The electronic absorption spectra of the investigated azo compounds **(LI-III)** in different organic solvents having different polarity and structures λ_{max}, are collected in, **Table (2)**. Exhibited irregular pattern of absorption maxima with change in polarity of the organic solvents. This anomalous trend can be considered to correspond to the net of several solvent effects such as polarity, basicity, Hydrogen bond and electron accepting ability. Other competing factors such as substituent effects or steric inhibition of resonance might be contributive. Electronic absorption spectra of **azo I** as for example, show in **Fig (1)**. The electronic absorption spectra of the compounds in solution exhibit three mainly bands, the first band in the range of 285 –301 nm which is attributed: **(π-π*)** (K band) electronic transition within aromatic ring **(18)**. Which observed in all solvents except acetone, Hexane and ethyl acetate this assignment is quite reasonable since λ_{max} of this band is slightly altered from one azo compound to another. The second band in the range (322-355nm) this band assigned to **(n-π*)** electronic transition of azo -N=N-, $C=O$**(19, 20)** and -*OH*groups, **Scheme (I)**.

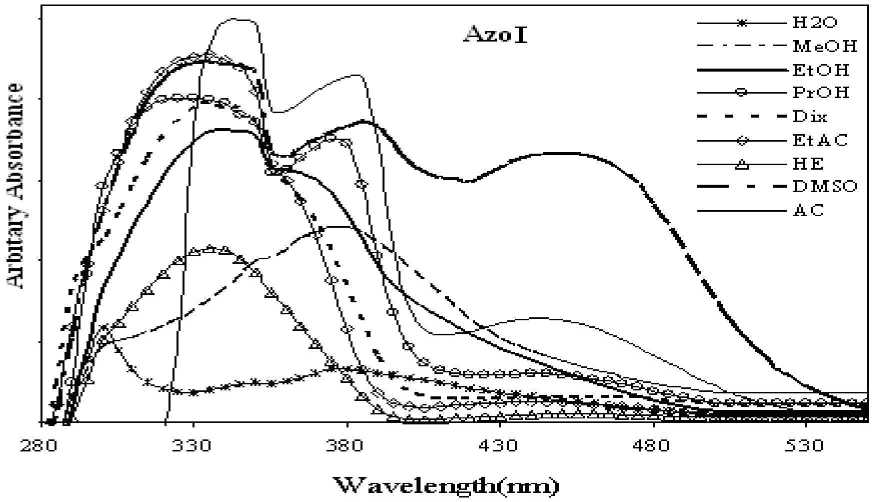

Fig.(1): Electronic Absorption Spectra of azo I in different solvents.

Third band in the range (361-403nm) and broad which is relative to intramolecular charge transfer *(CT transition)* (21). The charge-transfer nature of this band is deduced from its broadness as from the sensitivity of its λ_{max} to the type of substituent attached to the azo coupler. This band acquires an appreciable shift towards lower energy (***red shift***) when the substituents are electron acceptor as it compared with the cases where the substituents are electron donor (***blue shift***), (22). **Fig. (2)**. Charge transfer nature formed through the conjugation between the azo group and the aromatic ring system in which the azo group acts as a donor (23). **Azo I** compound exhibit an apparent shift towards longer wavelengths in different solvents according to the sequence :**Hexane< Ethyl acetate <1,4-Dioxane < Acetone< Ethanol<DMSO**. The shift agrees with the change in the polarity of the organic solvents and can be consider because of combination of several solvent characteristics such as polarity, basicity, and H-bond-accepting ability.

The λ_{max} shifts to longer wavelengths with increasing hydrogen bonding ability and polarity of the solvent. In the present study the **(π-π*)** band is red shifted when proceeding from the non polar solvent 1,4 Dioxane (e.g. **Azo I**: λ_{max} = 292 nm) to polar solvent H_2O (λ_{max} = 300nm)). This shift is mainly due to solute-solvent interactions that cause stabilization of the **π*** orbital more than the **π** orbital in polar solvents(24). All compounds possess an azo group conjugated to two arenes. The *trans* azo isomer possesses a lower steric hindrance compared to the *cis* isomer with possible azo-hydrazone tautomerism(15).

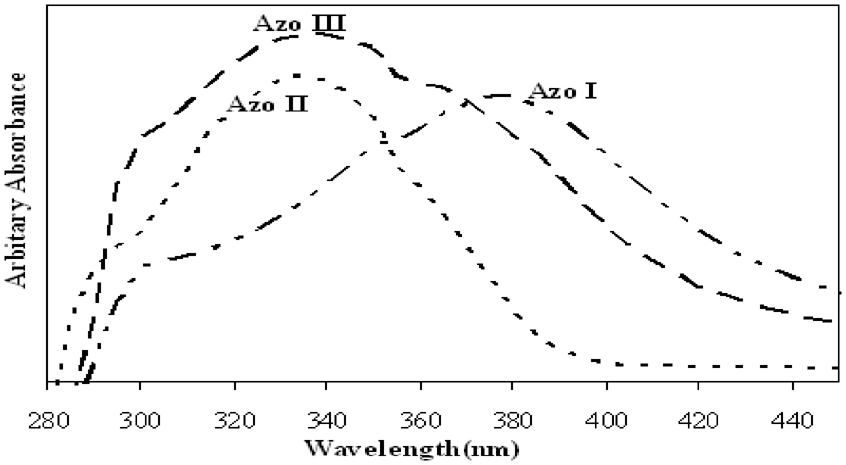

Fig.(2): Effect of position substituent on the electronic absorption spectra in MtOH.

All azo compounds were studies in this paper possess intramolecular hydrogen bonding; the strength of hydrogen bonding is dependent on the position and type of substituents. Thus, the intramolecular hydrogen bond between *–OH* moieties and *azo or* C=O groups. Furthermore, intermolecular hydrogen bond between *–OH* moieties and solvent molecules give rise to decreasing in intensity of **(n-π*)** transition $^{(25-26)}$. (e.g, the band at 450, 445 nm in DMSO) for **azo (I & II)**, respectively, is a result of an intermolecular CT transition. This transition involves an electron transfer from lone pair of electrons of the oxygen atom in DMSO to antibonding orbital of the OH groups $^{(27)}$.

Table(2): Electronic absorption spectra of the azo dyes in presence of different solvents (λ_{max}, nm).

Solvents / Compound	*HE*	*Dix*	*EtAC*	*EtOH*	*MtOH*	*PrOH*	*AC*	*DMSO*	*H_2O*
Azo I	-	292	-	-	300	-	-	-	300
	338	334	336	346	-	325	343	345	-
	-	364	361	370	375	375	380	385	379
	-	-	-	-	-	-	440(b)	450	-
Azo II	-	-	-	-	289(b)	289(b)	-	-	-
	329	331	334	322	338	328	352	335	-
		365(b)	365(b)	382	-	368	373	403	-
	-	-	-	-	-	-	-	445	-
	-	-	-	-	-	-	-	475	-
Azo III	-	295	-	300	299	301	-	300	-
	335	337	340	338	335	340	343	352	-
	-	375	381	367	373(b)	367	370	-	-
	-	-	-	-	-	-	-	489	-

[Where (b) = broad (azo II & III insoluble in H_2O)]

In comparing the spectral bands of azo I with azo II exhibited blue shift to shorter wavelength, see Table (2), which is attributed to the position of $-CH_3$ group to azo group. The presence of $-CH_3$ in ortho position to azo group lead to increasing the electronic density at azo group and decrease the energy of (n-π*) transitions relative to $-CH_3$ group in meta position in azo I. The proton accepting solvents lead to an increase in the aggregation of the molecules beside the intramolecular hydrogen bond. See scheme (II). The electronic spectral for Compound I in (DMSO) exhibited bands λ_{max} = 489nm, is assigned to the weak forbidden, (n-π*), transitions. Because the lone pairs of electrons of the nitrogen atoms and –OH moieties become free and participates in appearance of the (n-π*) transition (26).

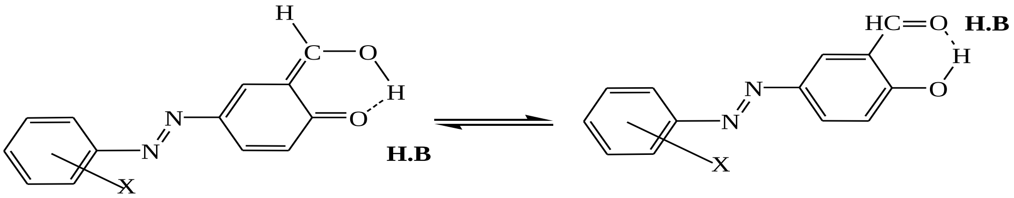

Scheme (II): Keto-enol tautomerism for azo (I, II)

The second spectral band of **azo III** is red shifted to longer wavelength compared with **azo II** as result formation of azo- hydrazone tautomerism form between azo group and *o-OH* group. **See scheme (III)**, stability of such structures depends on the solvent and the strength of such a hydrogen bond relative to that formed between the solute and solvent molecules and whether the azo or the hydrazone tautomerism dominate. Vice-versa, the third band exhibits hyposochromicity shift (e.g λ_{max} = 367nm in ethanol to λ_{max} =381nm in ethyl acetate). As solvent polarity increases, the ground state molecule is better stabilized.

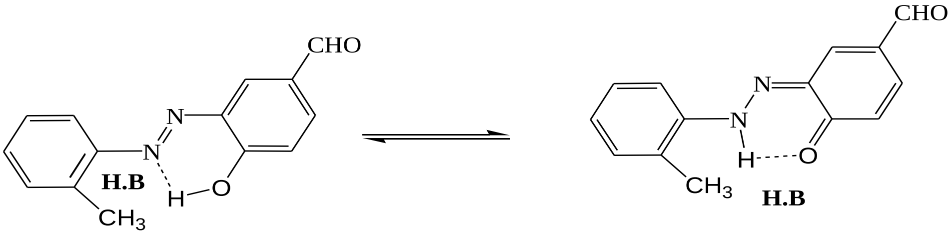

Scheme (III): Azo- Hydrazone tautomerism for azo III

MULTIPLE LINEAR REGRESSION ANALYSIS:

The maximum wavelength of absorption spectra (λ_{max}) was used in the following equation of multiple linear regression technique (28,29).

$$Y = a_o + a_1X_1 + a_2X_2 + a_3X_3 + \dots + a_nX_n \qquad (1)$$

Where *Y* is the peak maximum located on the absorption spectra in a given solvent; x_1, x_2, x_3, ..., has been expressed as a linear function using different combinations (one-, two-, three- and four) of solvent polarity parameters (*E, K, M, J, H* and *N*), X_n, by **Eq.(1)**

The regression intercept, a_o, has been assumed to be an estimate of the peak position for gas phase spectra. a_1, a_2... a_n *are* the solvent polarity parameters coefficients· Where *E* is the empirical solvent polarity, which is sensitive to both solvent–solute hydrogen bonding and to dipolar interactions. *K* is a measure of the polarity of the solvent *and M* is a measure of solute permanent dipole–solvent induced dipole interactions.

$$E = 2.895\text{x}10^{-3}\upsilon_{\max} \qquad \text{K} = \frac{\varepsilon - 1}{2\varepsilon + 1} \qquad M = \frac{n^2 - 1}{2n^2 + 1}$$

The functions *J* and *H* have been introduced to account for the nonspecific solute–solvent interactions such as dispersion and dipolar effects. *N* is a measure of permanent dipole–permanent dipole interactions

$$\text{J} = \frac{\varepsilon - 1}{\varepsilon + 2}, \qquad H = \frac{n^2 - 1}{n^2 + 2}, \qquad N = J - H$$

Regression analysis data for Y_1 and Y_2 bands (Y_1: λ_{max} ~ 285 to 301 nm and Y_2: λ_{max} ~ 329 to 405 nm) of the investigated compounds is given in **Tables (3a-5b)**. A value of *MCC* near to unity and / or a small value (near zero) of the significance parameter *(P)* mean the correlation is good. The analysis of the spectral shifts using one-parameter equation showed that all *MCC* values for all solvent parameters are very poor indicating difficulty of correlation for the studied spectral region Y_1 and Y_2. However, the parameter *K* gives a moderate correlation [*MCC* = 0.498 and 0.311 for **azo I** and **azo II** respectively] for the region Y_2, *i.e.* the dielectric constant (ε) of the solvent is the predominant parameter to explain the spectral shifts. On the other hand, **azo III** showed best *MCC* values (0.515) with parameter **M**, indicating relatively moderate contribution of solvent refractive index for region Y_1.

The regression analysis of the two-parameter equations improves the correlations. For the studied spectral region Y_1, The parameter **E** when combined with another parameter, either **N** or **K**, gave higher **MCC** values: 0.388and 0.318; 0.627 and 0.546 for **azo II** and **azo III**, respectively. Again, combining parameter **E** with two parameters *K, M or N*, better correlations (higher *MCC* values) were obtained. For example, (*K, M, E*), (*K, N, E*) and (*M, N, E*) for **azo II** (*o-*CH_3 substituents), **Tables (3a -3b)**, shows good fit compared to **azo I** (*m-*CH_3 substituents). Also, the combinations (*K, M, E*), (*K, N, E*) and (*M, N, E*) for **azo III** (*o*-OH), **Tables (5a -5b)**, show higher fit compared to **azo II** (*p-OH*), as result formation azo-hydrazo tautomersim, **Table (3a-5b)**. The four parameters combinations for all compounds showed the best fit of a value of *MCC* equals to ~ 1.000. This leads to the assumption that the combination of different solvent parameters *K, M, N* and *E* are effective to explain the spectral shifts depending on the electronic character of the substituent and the position of this substituent in the arene moiety of the studied hydroxy benzaldehyde azo dyes derivatives.

Table (3a): Regression analysis data for Y_1 bands for azo I dye.

Parameters	Y_1						
	a_0	a_1	a_2	a_3	a_4	MCC	P
K	332.481	14.788				0.063	0.586
M	330.730	38.553				0.010	0.869
N	335.227	6.732				0.075	0.553
E	335.809	0.055				0.003	0.902
K,M	325.644	14.693	35.747			0.069	0.867
K,N	363.905	-142.15	66.175			0.123	0.769
K,E	345.256	45.531	-0.583			0.160	0.706
M,N	327.208	41.602	6.778			0.082	0.843
M,E	328.214	39.161	0.057			0.006	0.981
N,E	358.182	22.609	-0.708			0.208	0.628
K,M,N	355.750	-221.91	125.776	99.664		0.172	0.886
K,M,E	340.551	45.099	23.797	-0.576		0.162	0.894
K,N,E	397.320	-181.02	100.115	-0.789		0.285	0.765
M,N,E	350.230	41.190	22.646	-0.708		0.215	0.843
K,M,N,E	389.612	-275.32	145.554	140.626	-0.830	0.349	0.878

Table (3b): Regression analysis data for Y_2 bands for azo I dye.

Parameters	Y_2						
	a_0	a_1	a_2	a_3	a_4	MCC	P
K	346.156	63.513				0.498	.0.050
M	356.698	90.278				0.036	0.651
N	360.200	23.883				0.488	0.054
E	354.825	0.393				0.195	0.273
K,M	298.553	77.236	222.223			0.695	0.051
K,N	344.977	68.938	-2.077			0.498	0.176
K,E	347.701	69.866	-0.090			0.503	0.174
M,N	305.537	268.057	31.715			0.757	0.029
M,E	282.441	304.092	0.715			0.478	0.197
N,E	366.749	30.095	-0.210			0.511	0.167
K,M,N	341.725	-295.071	410.116	146.981		0.858	0.036
K,M,E	283.916	62.961	270.926	0.244		0.724	0.129
K,N,E	376.822	-37.383	45.896	-0.268		0.512	0.365
M,N,E	297.703	287.673	28.652	0.123		0.763	0.093
K,M,N,E	404.226	-530.085	438.936	251.955	-0.529	0.911	0.063

Table (4a): Regression analysis data for Y_1 bands for azo II dye.

Parameters	Y_1						
	a_0	a_1	a_2	a_3	a_4	MCC	P
K	326.267	18.646				0.064	0.544
M	349.059	-81.500				0.021	0.729
N	329.991	7.770				0.066	0.539
E	336.312	-0.061				0.003	0.889
K,M	339.019	17.589	-65.120			0.078	0.816
K,N	332.087	-10.321	11.996			0.066	0.843
K,E	345.901	76.188	-0.967			0.318	0.384
M,N	340.956	-56.467	7.189			0.076	0.821
M,E	357.758	-100.301	-0.117			0.033	0.919
N,E	367.909	37.774	-1.186			0.388	0.293
K,M,N	335.291	54.765	-84.570	-15.527		0.080	0.946
K,M,E	388.735	87.420	-193.722	-1.209		0.422	0.488
K,N,E	419.450	-211.841	131.264	-1.453		0.465	0.428
M,N,E	403.562	-157.241	40.204	-1.347		0.459	0.436
K,M,N,E	423.330	-140.732	-93.413	101.326	-1.459	0.482	0.643

Table (4b): Regression analysis data for Y_2 bands for azo II dye.

Parameters	Y_2						
	a_0	a_1	a_2	a_3	a_4	MCC	P
K	342.175	81.440				0.311	0.251
M	265.575	571.166				0.383	0.190
N	360.195	31.297				0.291	0.269
E	338.551	0.851				0.141	0.463
K,M	207.991	96.828	661.001			0.813	0.081
K,N	276.374	388.670	-122.380			0.344	0.532
K,E	347.639	92.575	-0.229			0.315	0.567
M,N	223.223	687.489	39.332			0.828	0.072
M,E	197.964	658.599	1.153			0.633	0.222
N,E	369.220	36.621	-0.266			0.297	0.590
K,M,N	259.932	-221.397	742.887	127.518		0.841	0.229
K,M,E	206.331	94.200	662.731	0.055		0.813	0.266
K,N,E	263.142	424.568	-139.811	-1.453		0.345	0.797
M,N,E	226.537	685.952	41.088	-.0.089		0.828	0.246
K,M,N,E	291.933	-325.000	761.934	176.639	-0.397	0.850	0.552

Table (5a): Regression analysis data for Y_1 bands for azo III dye.

Parameters	Y_1						
	a_0	a_1	a_2	a_3	a_4	MCC	P
K	331.230	22.223				0.235	0.224
M	292.812	249.179				0.515	0.045
N	336.246	8.026				0.180	0.294
E	338.057	0.044				0.005	0.872
K,M	277.582	26.673	274.019			0.847	0.009
K,N	284.731	253.661	-95.8490			0.523	0.157
K,E	346.478	66.909	-0.7510			0.627	0.085
M,N	280.428	287.436	10.986			0.841	0.010
M,E	277.879	281.453	0.201			0.602	0.100
N,E	361.457	27.974	-0.7890			0.546	0.139
K,M,N	274.882	53.623	259.920	-11.256		0.850	0.040
K,M,E	296.990	53.932	223.819	-0.472		0.982	0.001
K,N,E	318.939	174.756	-49.149	-0.5690		0.680	0.170
M,N,E	305.397	247.245	24.153	-0.537		0.998	0.000
K,M,N,E	308.283	-20.549	256.565	33.078	-0.553	0.999	0.000

Table (5b): Regression analysis data for Y_2 bands for azo III dye.

Parameters	Y_2						
	a_0	a_1	a_2	a_3	a_4	MCC	P
K	383.894	-28.327				0.274	0.286
M	359.767	67.149				0.020	0.789
N	378.069	-11.491				0.309	0.252
E	391.492	-0.423				0.399	0.179
K,M	481.589	-69.542	-436.633			0.543	0.309
K,N	339.367	176.990	-78.796			0.407	0.475
K,E	391.377	-4.536	-.379			0.402	0.463
M,N	489.924	-549.323	-31.764			0.691	0.172
M,E	451.335	-261.326	-0.676			0.560	0.292
N,E	389.716	-2.565	-0.355			0.404	0.460
K,M,N	452.051	312.959	-699.405	-156.313		0.968	0.048
K,M,E	500.608	-45.243	-481.527	-0.455		0.723	0.385
K,N,E	360.553	112.275	-48.795	-0.214		0.429	0.719
M,N,E	500.829	-546.767	-22.914	-.348		0.782	0.308
K,M,N,E	446.417	339.205	-712.568	-168.753	0.078	0.971	0.255

SOLVENT INDUCED SPECTRAL DATA ANALYSIS BY TWO-PARAMETER EQUATION

Two-parameter equation was applied to further estimate the solvent induced spectral shifts (30).

$$\nu_{\text{solution}} = \nu_{\text{vapor}} + K_1\frac{2\varepsilon-2}{2\varepsilon+1} + K_2\frac{2n^2-2}{2n^2+1} \qquad (2)$$

Where $\nu_{solution}$ is the wavenumber of the peak maximum in presence of solvent, ν_{vapour} is the wavenumber of the peak maximum in absence of solvent, and K_1, K_2 and ν_{vapor} are the coefficients calculated using multiple regression technique. K_1, K_2, ν_{vapor}, r^2 (ν, ε), r^2 (ν, n) and MCC for the compounds **I-III** are calculated, collected in (**Table6**). The data indicate that both ε and **n** of solvents affect the electronic spectral properties of these compounds but with varying degree.

Table (6): Correlation analysis data for the compounds using the frequency of the absorption maximum (Y_2) in the presence of solvents from Eq (2).

Compounds	$\nu_{vapour}(cm^{-1})$	K_1	K_2	$r^2(\nu,\varepsilon)$	$r^2(\nu,n)$	*MCC*
Azo I	31653.49	-2332.43	-1961.77	0.714	0.114	0.803
Azo II	38031.96	-2829.17	-19219.78	0.566	0.604	0.895
Azo III	19132.78	1022.14	-2437.31	0.526	0.142	0.733

The K_1 and K_2 values are negative for aryl azo dyes .This indicates that strong solute–solvent interaction is taking place, and causing decrease in energy of electronic transition from **LUMO** to **HOMO** compared with the vapor state (31). On the other hand, the correlation data between **(**ν, n**)** is poor for **azo I**, and **azo III** and medium for **azo II**. The correlation data between **(**ν, ε**)** is poor for **azo III**, medium for **azo II** and good for **azo I**.

SOLVATOCHROMISM POLARITY SCALES COLLERATIONS

Kamlet-Taft's Method

The Kamlet–Taft's Eq. (3) (15) was used in order to describe in this case the overall solvent effects. **Eq. (3)** predicts the solvent effects and the interactions between solute and solvent molecules.

$$\nu_{\max} = \nu_0 + s\pi^* + a\alpha + b\beta \qquad (3)$$

In relation **(3)**, $\nu_{\max}$ is the wavenumber (cm^{-1}) in the maximum of absorption band of the dye dissolved in pure solvent; ν_0 is the regression intercept, which corresponds to the gaseous state of the spectrally active substance. The **Kamlet–Taft** solvent parameters π^*, α and β measure the solvent dipolarity/polarizability, the hydrogen bond donor acidity (**HBD**), and the hydrogen bond acceptor basicity (**HBA**) capabilities, respectively. The regression coefficients **s, a** and **b** are constants characteristic of the solute, their magnitudes and sign provide measures of the influence of the corresponding solute–solvent interactions on the wavenumber in the maximum of electronic absorption band.

Table (6).Multiple correlation coefficients for all samples from Kamlet–Taft equation.

Compounds	*Intercept ^10^3*	*a^10^3*	*b^10^3*	*s^10^3*	*R*	*n*
Azo I	29.051	0.0454	-1.5892	-1.945	0.848	**6**
Azo II	30.618	-1.555	0.8001	-6.284	0.951	**6**
Azo III	24.309	-0.141	2.1480	2.357	0.861	**5**

The correlation coefficients, **R**, is greater than 0.55 for linear solvation energy relationship (**LSER**), showing a high quality of the multiparametric **Eq. (3)**. The coefficients **s, a** and **b** from **Eq. (3)**, (**Table (6)**), can indicate the strength of the different solute–solvent interactions.

From **Table (6)**, it can be observed that the most important contributions to the solvatochromism shift arise from dipolarity/ polarizability (**π*** term) is much more pronounced than that of hydrogen bond accepting ability (β term). The effect of α term on the solvatochromism shift is practically negligible, the negative sign of **s** coefficient, for **azo** (**I** & **II**) shows a positive solvatochromism with both increasing solvent dipolarity/polarizability (**π***). This suggests a higher stabilization of the electronic excited state as compared to the ground state stabilization. The positive sign of ***b*** coefficient and negative sign of **a** coefficient suggest the formation of solute–solvent hydrogen bonds for both electronic states, which stabilizes them in solvents with high hydrogen bond donating and low hydrogen bond accepting abilities. It is worth noting that the **b** coefficients are significantly smaller than the **a** coefficients for the calculated linear solvation energy relationship (**LSER**). The very small value of ***a*** coefficient demonstrates that the ability of the azo dyes **(I & III)** to donate hydrogen bonds have *a* smaller influence on $\boldsymbol{\nu}_{\mathbf{max}}$ compared with their ability to accept hydrogen bonds. The positive sign of **b** coefficient for **azo III** that indicates a hypsochromic shifts with increasing solvent hydrogen bond basicity. This indicates the stabilization of the ground state relative to the electronic excited state.

The contribution of each parameter to solvatochromism, on a percentage basis, was calculated from the values of regression coefficients it is given in **Fig. (3)**. From these results, one can observe that the contribution of the solute–solvent dipole–dipole interactions (**π***) to bathochromic shift is much more pronounced than that corresponding to the specific ones (**α** and **β**). Thus, the values obtained for percentage contributions of calculated solvatochromic parameters (**Fig. (3)**) show that a major contribution to the solvatochromism is due to the solvent dipolarity/polarizability (non-specific solute–solvent interactions) for all studied dyes, (%▯* =54.19, 72.39,and 48.69%) respectively. This effect is dependent on the position of the strong electron donating substituents (CH_3 and OH).

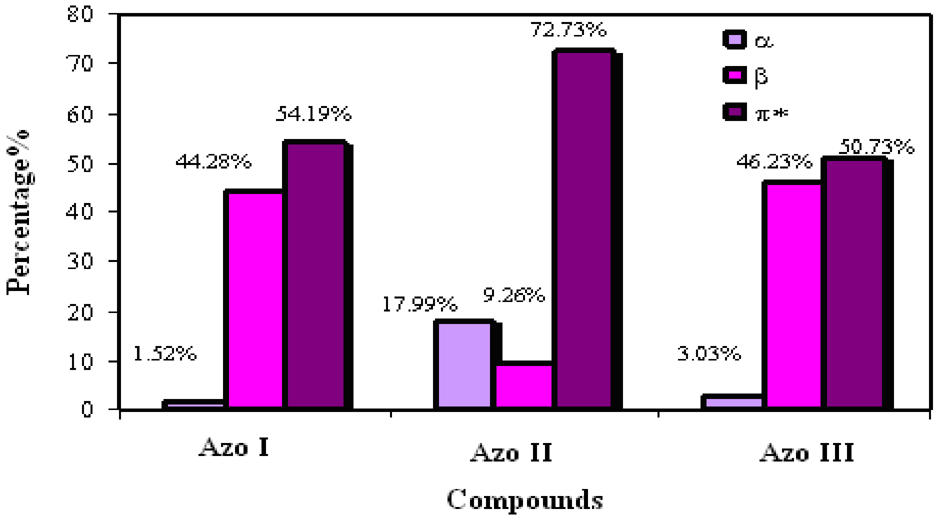

Fig. (3) Contribution of solvatochromic parameters from Eq (3).

The sign of absorption solvatochromism for each compound can be obtained by subtracting the ν_{max} in the most polar solvent from that determined in the most non-polar solvent and it is considered as a spectral shift, $\Delta\nu$ (**Table7**). Red or blue spectral shifts can be indicated from the positive and negative signs of $\Delta\nu$, respectively (32,33). All investigated compounds exhibited a positive absorption solvatochromism on increasing the solvent polarity (**Table 7**) except **Azo III**. This was attributed to hydrogen bonding between electron pair of nitrogen atom and the polar solvents in the investigated compounds. Correlation was made between the predicted absorbance maxima (ν_{max}) calculated from the **Kamlet-Taft** equation and the experimental (ν_{max}) values in order to assure the quality and applicability of the equation, **Figs. (5a-7a)**, this is proved by the results of **R**^{2} values of compound **I** (0.719); compound **II** (0.905) and compound **III** (0.741).

Table (7): Solvatochromism of Azo Dyes.

Compounds	*$\nu_{1max}(cm^{-1}).10^3$ A polar solvent*	*$\nu_{1max}(cm^{-1}).10^3$ polar solvent*	*$\Delta v.10^3$*	*Solvatochromism*
Azo I	26.315	27.472	1.157	+
Azo II	26.809	27.397	0.588	+
Azo III	27.027	26.881	-0.146	-

Catalân Method

More recently, the polarity scale (**π***) proposed by **Kamlet** and **Taft** has been further separated by Catalân into two independent parameters: solvent polarizability (**SP**) and dipolarity (**SdP**) scales (**see Eq. (4)**) (16, 17):

$$\nu_{max} = \nu_0 + C_{SP}SP + C_{SdP}SdP + C_{SA}SA + C_{SB}SB \qquad (4)$$

Where **SP** denotes solvent polarizability, **SdP** – solvent dipolarity, **SA** – solvent's hydrogen bond donor strength and **SB** – hydrogen bond acceptor strength. It has been also demonstrated that **Catalân** model offers better statistics when describing the solvatochromism of azo dyes in comparison to the **Kamlet-Taft** model (34).

Table (8): Multiple correlation coefficients for all Compounds from Catalân equation.

Compounds	*Intercept ^10^3*	*$C_{SP}^{10}^3$*	*$C_{SdP}^{10}^3$*	*$C_{SA}^{10}^3$*	*$C_{SB}^{10}^3$*	*R*	*n*
Azo I	30.443	-2.7640	-2.1665	-0.0392	-0.1505	0.913	6
Azo II	34.022	-10.542	-2.9353	-3.8032	4.373	0.970	6
Azo III	13.932	15.303	2.7580	0.8150	1.291	0.916	4

.

Moreover, the multiparametric regression analysis according to **Catalân Eq. (4)** showed negative sign of C_{SA} coefficient and C_{SP} coefficient for arylazo dyes (**I & II**) (**Table(8)**). This indicates a bathochromic shifts with an increasing solvent hydrogen-bond acidity and solvent polarizability (35). The positive sign of C_{SB} coefficient, and C_{SP} coefficient for aryl azo dyes **III**, this indicates a hypsochromic shifts with increasing solvent hydrogen-bond acceptor basicity and solvent polarizability. The negative sign of C_{SdB} coefficient indicates a bathochromic shifts with increasing solvent dipolarity. The percentage contribution of solvatochromic parameters (**Fig. (4)**) for all azo dyes showed that solvent polarizability is the most important parameter, which influences the absorption frequency shifts. Solvent hydrogen-bond basicity and dipolarity have a moderate influence on solvatochromism, whereby the effect of solvent dipolarity has a more significant impact compared with the solvent basicity for aryl azo dyes **I & III**. However, for **azo II** the value of S_B is a highest and consequently, the solvatochromic behavior of this dye will be governed by hydrogen bond interaction. Solvent acidity has a negligible impact on solvatochromism.

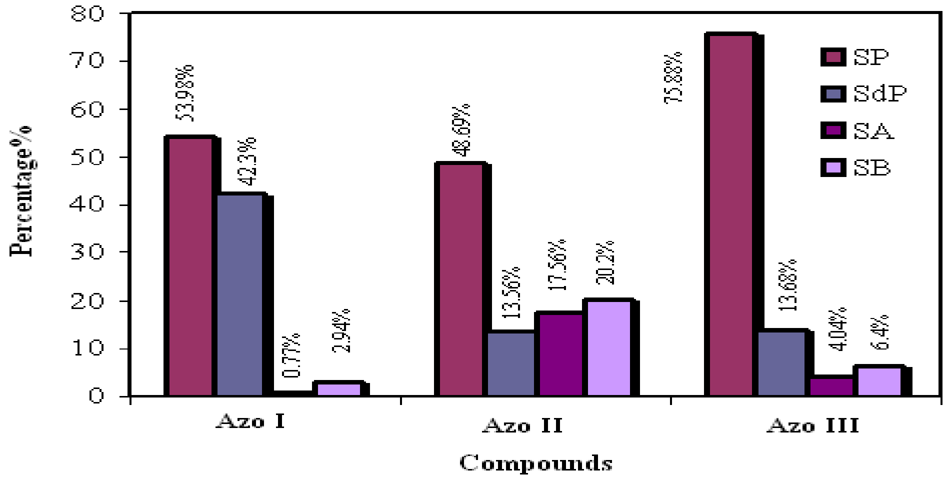

Fig. (4) Contribution of solvatochromic parameters from Eq.(4).

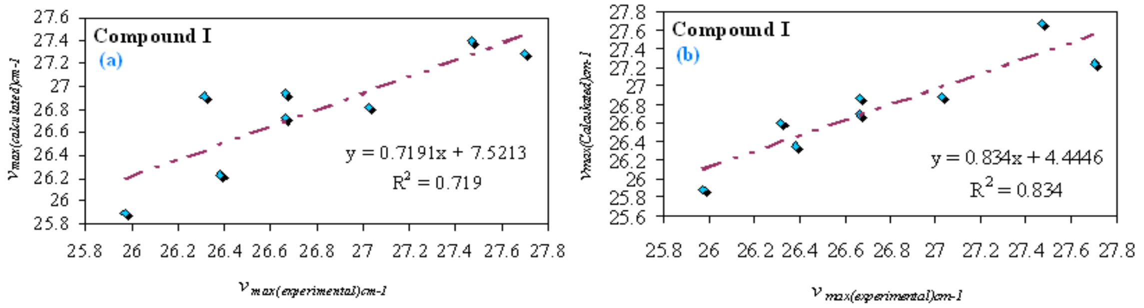

Fig (5) Plot of calculated absorption maxima versus experimental values for Azo I in different solvents using (a) Kamlet–Taft's method, Eq. (3), (b) Catalân's method, Eq. (4).

The Catalân model has successfully predicted the negative coefficients associated with $\mathbf{S_A}$ and $\mathbf{S_B}$ parameters indicating that hydrogen bond formed by azo compounds and protic solvents stabilize the excited state rather than the ground state, resulting in bathochromic shift(36), (e.g azo **I** & azo **II**). Correlation was made between the predicted absorbance maxima (ν_{max}) calculated from the Catalân equation and the experimental (ν_{max}) values in order to assure the quality and applicability of the equation, **See Fig (5b-7b).** This is proved by the results of $\mathbf{R}^2$ values of compound **I** (0.834); compound **II** (0.9414) and compound **III** (0.8387); **Figs (.5b-7b).**

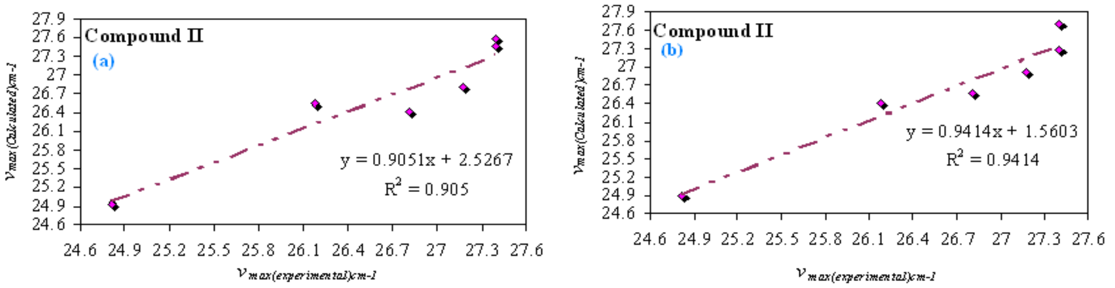

Fig (6) Plot of calculated absorption maxima versus experimental values for Azo II in different solvents using (a) Kamlet–Taft's method, Eq. (3), (b) Catalân's method, Eq. (4).

From the results, The **Kamlet-Taft** and **Catalân** solvent scales were found to be the most suitable for describing the solvatochromic shifts of the electronic absorption band. The adjusted coefficient representing the electron releasing ability or basicity of the solvent, b or C_{SB} has a negative value, suggesting that the absorption bands shift to lower energies with the increasing electron-donating ability of the solvent. This effect can be interpreted in terms of the stabilization of the resonance structures of the chromophore(37).

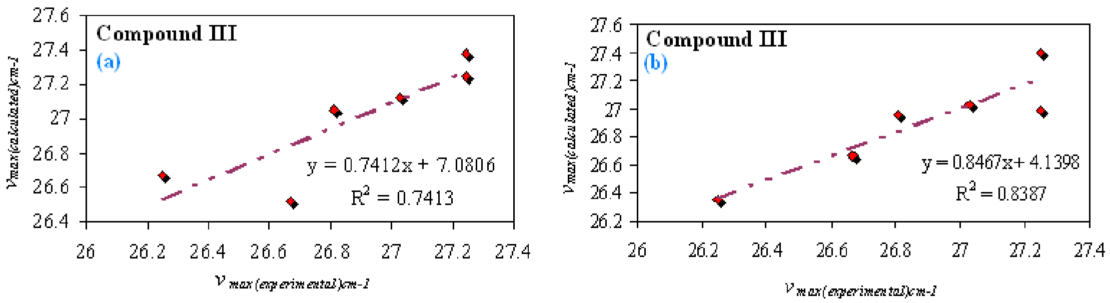

Fig (7) Plot of calculated absorption maxima versus experimental values for Azo III in different solvents using (a) Kamlet–Taft's method, Eq. (3), (b) Catalân's method, Eq. (4).

CONCULSIONS:

Azo dyes have been synthesized and characterized. Measurements of absorption spectra in various organic solvents, showed moderate to high solvatochromism. Multiple linear regression techniques were used to evaluate the effects of solvent polarity and hydrogen bonding on the spectra. **Kamlet-Taft** and **Catalân** equations with the parameters (**π^*, β, α**) and (**SP, SdP, SA, SB**) were useful to demonstrate the effects of both types of hydrogen bonding and solvent dipolarity/polarizability. Positive solvatochromism is observed in all compounds (except azo III) with increasing solvent polarity. This study can provide valuable information concerning reactivity and spectroscopic characteristics of studied molecules.

RECOMMENDATIONS

The study recommend by the following: studying effect of mixture solvents on these compounds, effect of antibacterial and preparation complexes with different transition metals.

LIST OF ABBREVIATION

Name	*Abbreviation*	*Name*	*Abbreviation*
Solvent dipolarity	*SdP*	*1,4-Dioxane*	*Dix*
Solvent polarizability	*SP*	*Ethanol*	*EtOH*
Solvent acidity	*SA*	*Methanol*	*MtOH*
Solvent basicity	*SB*	*n-Hexane*	*HE*
dipolarity/ polarizability	π^*	*Ethyl Acetate*	*EtAc*
hydrogen bond accepting basicity	β	*Water*	H_2O
hydrogen bond donor acidity	α	*Acetone*	*Ac*
Dimethyl Sulfoxide	*DMSO*	*1-Propanol*	*PrOH*
Wave length	λ_{max}	*Wave number*	ν_{max}

REFERENCE

1. Aljamali. N; Biochem Anal Biochem 4(2) (2015)1.
2. Gouda,M.;& Abu-Hashem,A.; *Arch. Pharm.* 344(3)(2011)170.
3. Zakerhamidi, M. ; Keshavarz, M. ; Tajalli, H. ; Ghanadzadeh, A. ; Ahmad, S. ; Moghadam, M.; Hosseini, S. & Hooshangi, V. , J. Mole. Liq. 154 (2010) 94
4. Khatua, P. ; Ghosh, S. & Bhattacharya, S. , *J. Oleo Sci.* 52(7) (2003)387.
5. Uscumlic, G. & Nikolic, J. , *J. Serb. Chem. Soc.* 74 (2009) 1335.
6. Airinei, A. ; Homocianu, M. & Dorohoi, D. , *J. Mole. Liq.* 157 (2010) 13.
7. Airinei, A. ; Rusu E. & Dorohoi, D. , Solvent influence on the electronic absorption spectra of some azoaromatic compounds. Spectrosc Lett 34(1) (2001) 65.
8. Reichardt, C. , Solvents and Solvent Effects in Organic Chemistry, 3 rd ed., Weinheim Wiley-VCH, (2003).
9. Pagariya, R; & Thakare, N.; *Res. Arti* 8(5)(2016)385.
10. Al Jebaly, A. ; Gheath, A. & Habib, I. Synthesis , Potentiometric and Spectro- Photometric studies of some hydroxy benzaldehyde azo dyes with copper, iron ions Benghazi Univ. Fac. Sci., Chemistry Program, Master of Science Thesis; January (2013) 12.
11. Rauf, M.; Soliman, A. & Khattab, M.; Chem. Cen. J. 19(2)(2008)1.
12. Behera P.; Xess A.; & Sahu S.; Bull. Korean. Chem. Soc. 35(2)(2014) 610.
13. Masoud, M.; Ali, A.; Shaker, M.; & Abdul Ghani, M.; *Spectrochim. Acta A* 60 (2004)3155; 61(2005)3102.
14. Al Jebaly, A.; Hemdan, S.; & Ali, F; J. Human. Sci. 39(2017) 1.
15. Masoud, M. ; Elsamra, R.;& Hemdan, S.;J. Serb. Chem. Soc.82(7-8)(2017)1.
16. Catalân, J. , *J. Phys. Chem. B* 113 (2009) 5951.
17. delValle, J. ; Garcia Blanco, F. & Catalân, J. , *J. Phys. Chem. B* 119 (2015) 4683.
18. Abou El-Enein, S. & El-Mallah, N., *Afinidad 1L*, 440, (1992) 269.
19. Masoud, M.; Hindawy , A. ; El-Dissouky , A. ; Mohamed, G. & Abd El –Fattah, T. Egypt J. Chem. 35, (1992) 183.
20. Masoud, M.; Hafez, O. & Soayed, A. *Bull Fac. Sci., Assiut Univ.*, 24B (1995) 34.
21. Masoud, M.; Haggag, S. & Hassan, O. ,*Rev. Roum. Chim*, 41(1995)21.
22. Dakiky, M. ; Kanan, K. & Khamis, K. , *Dyes Pig.* 41, (1999) 199.
23. Syhood, A.; & Mohammed, H.; *Inter. J. Sci. Res.*4(6)(2013)504.
24. Hammud, H.; Bouhadir, K.; Masoud, M.; Ghannoum, A. & Assi, S., J. Solution Chem. 37(2008) 895.
25. Gulseven, Y. ; Tasal, E.; Sıdır, I.; Gungor, T.; Berber, H. & Ogretir, C. , Int. J. Hydrogen Energy 34(12) (2009) 5255; 34(12) (2009) 5267.
26. Sıdır, Y.; Sıdır, I.; Tasal, E. & Ermis, E., *Spectrochimica Acta Part A* 78 (2011) 640.
27. Alizadeh, K.; Seyyedi, S.; Shamsipur, M.; Rouhani, S. & Haghbeen, K., *Spectrochim. Acta A* 74 (2009) 691.
28. Costinela-Laura, G.; Ioan, P. & Ioan, B., *Dyes Pig.* 76(2) (2008)455.

29. Hammud, H.; Ghannoum, A. & Masoud, M., Spectrochim. Acta A 63(2) (2006)255; 57(2001)977.
30. Hammud, H.; Ghannoum, A.; Fares, F.; Abramian, L. & Bouhadir, K., *J. Mol. Struct.* 881(2008) 11.
31. Hammud, H.; El-Dakdouki, M.; Sonji, N. & Bouhadir, K. , European J. Chem. 6 (3) (2015) 325.
32. Rusu, E.; Dorohoi, D. & Airinei, A., *J. Mol. Struct.* 887(2008) 216.
33. Masoud, M.; Shaker, M.; Ali, A. & Elasal, G., *Spectrochim. Acta A 79*(2011)538.
34. Filarowski, M.; Kluba, M.; Cie´slik-Boczula, K.; Koll, A.; Kochel, A.; Pandey, L.; De Borggraeve, W.; Vander Auweraer, M. ; Catalân, J. & Boens, N., *Photochem. Photobiol. Sci.* 9 (2010) 996.
35. Alimmari, A.; B.Bozic, B.; Mijin, D.; Marinkovic, A.; Valentic, N. & Uscumlic , G. *Arabian J. Chem.* 8 (2015)269.
36. Miotke, M. & Jozefowicz, M., *J. Mole. Liq.* 230 (2017) 129.
37. Jayabharathi, J.; Thanikachalam, V.; Devi, K. & Perumal, M. , J. Fluorescence 22(2)(2012)737.

الملخص: درست أطياف الامتصاص الالكترونية للمركبات الازو فى الماء والمذيبات العضوية مختلفة القطبية عند درجة حرارة الغرفة وفسرت الانتقالات الالكترونية كما درست تاثيرات المذيبات على السلوك الطيفى ونوقشت . حللت كذلك التأثيرات الطيفية للمذيب باستخدام تقنية الانحدار الخطى المتعدد .

الكلمات المفتاحية: مركبات الازو ، أطياف مرئية ،مذيبات ، تقنية الانحدار الخطى المتعدد.
